Regular Article

PHYSICAL CHEMISTRY RESEARCH
Published by the
Iranian Chemical Society
www.physchemres.org
info@physchemres.org

Phys. Chem. Res., Vol. 12, No. 4, 963-974, December 2024
DOI: 10.22036/pcr.2024.433628.2466

Computational Investigation of Potent EGFR Inhibitors from Flavonoid-Based Phytochemical Constituents of *Caralluma Europaea* as Pancreatic Cancer Agents

K. El Khatabi[a], M. Alaqarbeh[b,*], H.M. Rehman[c], M.A. Ajana[a], T. Lakhlifi[a] and M. Bouachrine[a]

[a]*Molecular Chemistry and Natural Substances Laboratory, Faculty of Science, University Moulay Ismail, Meknes, Morocco*

[b]*Basic Science Department, Prince Al Hussein bin Abdullah II Academy for Civil Protection, Al-Balqa Applied University, Al-Salt 19117, Jordan*

[c]*School of Biochemistry and Biotechnology, University of the Punjab, Lahore, Pakistan*

(Received 2 January 2024, Accepted 16 July 2024)

The present study aims to identify effective bioactive compounds from Caralluma europaea as potential inhibitors of EGFR. Five Caralluma europaea compounds previously evaluated for their ability to inhibit cell proliferation were tested against EGFR and compared to the industry standard inhibitor Erlotinib. In this instance, these derivatives were focused on docking studies, which discovered the specific interactions of the identified phytocompounds with EGFR. Among the compounds, Hesperetin, Quercetin, and Myricetin demonstrated the highest total scores and the most favorable energies (lowest energy levels), attributed to their interactions with EGFR. These three phytochemical compounds may have a greater inhibitory potential for the EGFR than the reference control, Erlotinib. Thus, Hesperetin was able to dock deeply within the EGFR binding region, resulting in improved total scores and favorable binding interaction as well as docking energies, which were crucial in stabilizing the docking complex conformation. The results showed that Hesperetin had an excellent ADMET profile. The current findings forecast that the natural compound Hesperetin could be a better drug candidate for pancreatic cancer and non-small cell lung cancer. Further studies conducted in laboratory settings and within living organisms may illustrate its potential as a therapeutic option.

Keywords: Caralluma europaea, EGFR, Phytochemicals, Molecular docking, Molecular dynamics simulation, *In silico* ADMET

INTRODUCTION

Protein kinases play a central role in the aberrant signaling that characterizes the uncontrolled growth and spread of human tumors [1]. Loss of the delicate balance between cell proliferation and apoptosis results in it making it harder for damaged cells to be eliminated through apoptosis" for clarity and smoother flow [2]. Activating apoptotic pathways in tumor cells is a vital strategy for cancer treatment [3]. The regulation of cellular function heavily relies on growth factor signaling pathways, including metastasis, differentiation, survival, and cell proliferation [4].

*Corresponding author. E-mail: marwa.aqarbeh@bau.edu.jo

Epidermal growth factor receptor (EGFR) kinase is one of the growth factor receptor kinases that has been identified as being crucial in cancer [5]. The EGFR, which is implicated in the regulation of several important processes, is one of the most thoroughly studied receptors in hormone-refractory prostate cancer [6], lung cancer (especially lung adenocarcinomas) [7], and breast cancer [8]. Hence, the EGFR kinases represent promising targets for the development of novel cancer therapies [9]. There is a pressing need to develop new drugs to treat cancers caused by EGFR mutations [10]. Treatment of cancer using plant-derived products is a promising new alternative for treating this deadly disease [11]. Natural products are a great source for identifying and developing novel cancer therapy

alternatives, as the majority of anticancer medicines are of natural origin [12]. Therefore, plant-derived EGFR inhibitors might be promising options for cancer treatment [13]. Caralluma europaea, a member of the Apocynaceae family, is known for its various medicinal properties, including neuroprotective, antiatherosclerotic, antinociceptive, anti-inflammatory, antihyperglycemic, antiobesogenic, antiulcer, and antitrypanosomal activities [14]. To identify novel, potent antiproliferative drugs from Caralluma europaea, we conducted in silico studies on various structurally related polyphenols and flavonoids. Additionally, the probable mechanism of action of these metabolites was investigated by inhibiting EGFR.

MATERIALS AND METHODS

Experimental Data

Ligands. From the literature, a dataset comprising five phytocompounds sourced from Caralluma europaea, previously examined for their antioxidant and antiproliferative properties, was retrieved [15]. The selected phytocompounds were identified *via* HPLC by Amrati *et al.* and assessed for antiproliferative activity against cancerous cells using WST-1. The structures of the five reported phytocompounds and the standard inhibitor Erlotinib reported as antiproliferative agents are shown in Fig. 1.

Energy minimization and optimization. Gaussian software was employed to draw the three-dimensional (3D) structures of the reported phytocompounds acting as ligands (09, Gaussian Inc., Wallingford, CT, USA). The DFT approach was applied in combination with a basis set of B3LYP/6-311(d,p) levels to achieve the equilibrium geometry of each compound [16].

Receptor. The protein databank provided the EGFR protein crystal structure (PDB code: 1M17, resolution: 2.60), which was used in the present study [17]. The 1M17 protein is classified as a transferase protein and contains one chain A in complex with a 4-anilinoquinazoline inhibitor. This chain, which has 333 sequences, was utilized to prepare the macromolecule. The protein structure was prepared by removing the water, adding polar hydrogens, and then minimizing energy using the default settings [18]. Overall, the protein structure 1M17 appears to be of good quality, with no major issues that would significantly impact its reliability

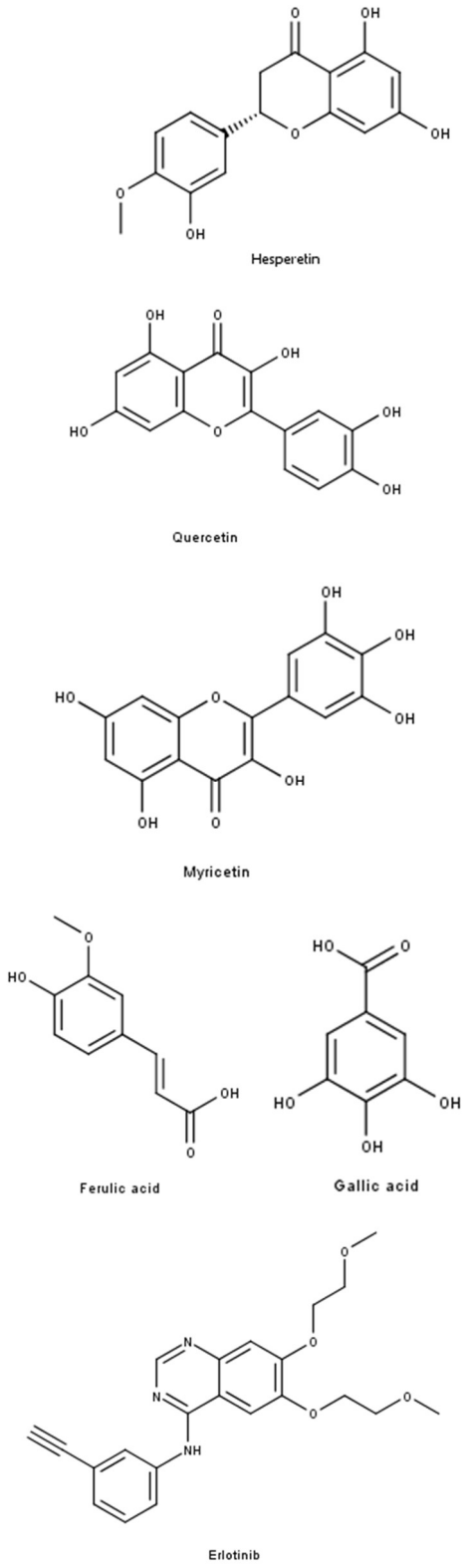

Fig. 1. Structures of the 5 reported Caralluma europaea-derived phytocompounds and Erlotinib.

for molecular docking studies. However, as with any structural analysis, it is important to consider the limitations of the resolution and any potential artifacts that may arise from the experimental technique used to determine the structure.

Molecular Docking Studies

Rapid protein-ligand docking. The PyRx AutoDock Vina approach was used for preliminary docking [19]. for molecular docking and virtual screening. The screened compounds were subsequently docked utilizing the iGEMDOCK 2.1 program to validate the outcomes of the AutoDock Vina docking values of chosen ligands. For identifying lead phytocompounds, iGEMDOCK is an effective drug design method. iGEMDOCK has provided the output with electrostatic, hydrogen bond, and Van Der Waals forces. For each protein-ligand docking, an average of 2 trials were used to ensure accuracy. With two solutions and a population size of 200, docking was performed. The generations parameter was set at 70. Thus, binding affinity values were acquired and utilized to assess the outcome of the docking process.

Molecular docking analysis. The molecular docking method is a powerful approach to investigating the probable binding mode of a ligand and understanding the structural interaction between a ligand and its protein [20,21]. The study utilized the Surflex-Dock module in SYBYL [22]. The reliability of this method was demonstrated by redocking the co-crystallized drug from the binding site [23]. The docking procedure proved trustworthy and may be applied in current investigations since the RMSD between the docked conformation and co-crystal of 1M17 was less than 2. In addition, the overall Surflex-Dock score, which represents binding force, was developed. A high binding affinity is implied by an increased total score. The results of the statistical docking were evaluated using a total score and binding affinity. The five phytochemicals were docked with the protein's pocket, and the interactions between the ligands and the protein were described and analyzed. DrugBank (www.drugbank.ca) provided the available approved drug (Erlotinib) for pancreatic cancer and non-small cell lung cancer, and it docked with the identical pocket of the targeted protein. Discovery Studio 2016 and PyMOL software were used to carry out the docking analyses [24,25]. Consequently, the total score and binding affinity were used to evaluate the docked findings.

ADMET Prediction

The early prediction of ADME and Toxicity of a novel ligand aids in lowering the probability of failure during the drug development phase and assessing promising molecules for clinical trials [26]. Using the pKCSM online tool, the ADMET properties of the four chosen compounds were predicted [27].

Molecular Dynamics Simulation

Molecular dynamics (MD) simulation is a robust computational method utilized to investigate the characteristics and behavior of molecules and materials on an atomic scale [28]. Desmond, a software package developed by D. E. Shaw, is designed for MD simulations of biological systems such as membranes and nucleic acids as well as proteins. The stability of protein-ligand interactions was assessed through MD simulations, with particular attention given to the most stable complexes that demonstrated high binding energies. Desmond was used to assess the dynamic binding behavior and stability of protein-inhibitor complexes in their docked states. The protein-protein complex underwent preprocessing with Maestro's Protein Preparation Wizard, which involved optimizing and minimizing the complex. All systems were set up using the System Builder tool. The complexes were solvated with the simple point-charge (SPC) water model within an orthorhombic box, ensuring a 10-Å buffer from the box edge, and were neutralized using $Na^{+/}Cl^{-}$ ions. To simulate physiological conditions, 0.15 M sodium chloride (NaCl) was incorporated. The potential energy of the protein complex was minimized within the NPT ensemble framework. The simulations were executed at 300 K and 1 atm pressure for a duration of 100 ns, employing the OPLS4 force field for NPT production. The models underwent relaxation prior to simulation. Short-range electrostatic interactions were determined using the particle mesh Ewald method, with a 9.0 Å cutoff radius for Coulomb interactions. Water molecules were explicitly represented by the simple point charge model. The Martyna–Tuckerman–Klein chain coupling scheme, with a coupling constant of 2.0 ps, managed pressure control, while the Nosé-Hoover chain

coupling scheme handled temperature regulation. Trajectories were saved every 100 ps for subsequent analysis, and the stability of the simulation was evaluated by monitoring the RMSD of the protein complex throughout the simulation period. Conformational changes from the initial structure throughout the simulation were expressed as RMSD and RMSF. A detailed description of the methodology is available elsewhere [29-31].

RESULTS AND DISCUSSION

Docking Analysis

A molecular docking method was performed to screen the query ligands and reveal their detailed interactions with the EGFR protein. The five compounds were docked into the EGFR protein's binding site, and their affinity was assessed, along with the reference drug Erlotinib. The binding affinity, total score, binding types, and active amino acid residues of the six compounds in the target protein were investigated. Table 1 shows the binding affinity and total score values of the five phytocompounds and Erlotinib.

Three phytocompounds (Hesperetin, Quercetin, and Myricetin) were shown to have the highest total scores and the best energies (lowest energy level) among compounds coming from the contribution of several interactions with EGFR. These three phytochemical compounds may have a greater inhibitory potential for the EGFR than the reference control, Erlotinib. As a result, the binding conformations between the targeted protein and the three chosen phytocompounds were further prioritized, thoroughly examined, and compared to the Erlotinib-protein binding conformations as shown in Figs. 2A, 2B, 2C, and 2D, respectively.

Further docking analysis revealed hydrogen bond interactions for the Hesperetin binding process, as depicted in Fig. 1A. A hydrogen bond was generated with the residue at Thr830. Another pivotal carbon-hydrogen bond between the phenyl located to the left of the compound and Thr766 was observed. These hydrogen bond and carbon-hydrogen bond interactions influenced the activity of Hesperetin and provided a guarantee for the stable binding of this phytocompound to the EGFR. π-sigma interactions, a type of hydrophobic interaction, were found between the right phenyl ring and Leu694 and Val702. Other hydrophobic contacts, including Leu820, Cys751, Thr766, and Ala719, can also be observed. The stability of Hesperetin's binding to the protein is significantly enhanced by the combined interactions. As illustrated in Fig. 2B, the docking conformation of Quercetin provided hydrophobic and hydrogen bonding interactions, among others. There were three hydrogen bonds involved with the active amino acid residues Thr766, Gln767, and Pro770, which are beneficial to the binding of Quercetin to the EGFR active site. Quercetin is found to be inserted into a hydrophobic pocket formed by key residues Ala719, Leu820, and Leu694. Additionally, the binding process includes two unfavorable donor-donor interactions with the amino residues Cys773 and Met769. Figure 2C shows the active site of EGFR, where Myricetin exhibited the lowest binding affinity of -8.7 and -97.73, as determined by AutoDock Vina and iGEMDOCK, respectively. The docking results indicate that Myricetin achieved the highest total score of 5.6081 and is positioned deep within the EGFR site, stabilized by three hydrogen bond interactions with residues Thr766, Asp831, and Thr830. It is also important to note that Myricetin interacts with Val702 to form a π-alkyl contact, which results in a hydrophobic

Table 1. Binding Affinity and TTotal Score Values of the 5 Selected Phytocompounds and Erlotinib

Phytochemical	AutoDock vina/PyRx Binding affinity (Kcal mol^{-1})	iGEMDOCK Binding affinity (Kcal mol^{-1})	Surflex-Dock Total score
Hesperetin	-8.3	-92.52	3.6198
Quercetin	-8.5	-97.05	5.4360
Myricetin	-8.7	-97.73	5.6081
Ferulic acid	-5.7	-72.19	2.9858
Gallic acid	-5.2	-79.37	2.8750
Erlotinib	-7.3	-81.03	2.5904

interaction. The docking conformation of Erlotinib, which has the highest binding affinity and the lowest total score values compared to the other three phytocompounds, was not able to provide any hydrogen bonds, as displayed in Fig. 2D. Carbon-hydrogen interactions were generated with the amino active residues Thr766, Thr830, Glu738, and Asp831Erlotinib engages in hydrophobic interactions, with π-sigma interactions involving its phenyl and naphthalene moieties with residues Leu694 and Val702, respectively, enhancing the binding. Additional hydrophobic interactions, including π-alkyl and alkyl interactions, were also observed. Remarkably, the interactions that are generated are stabilizing and beneficial to the efficacy of EGFR inhibitors. As with Erlotinib, the three phytocompounds also entered the EGFR cavity, resulting in improved total scores, docking energies, and favorable binding interactions that were crucial for maintaining the conformations of the docking complex. The docking results suggest that the three phytochemical compounds, particularly Hesperetin, could potentially be further developed to become novel EGFR inhibitors.

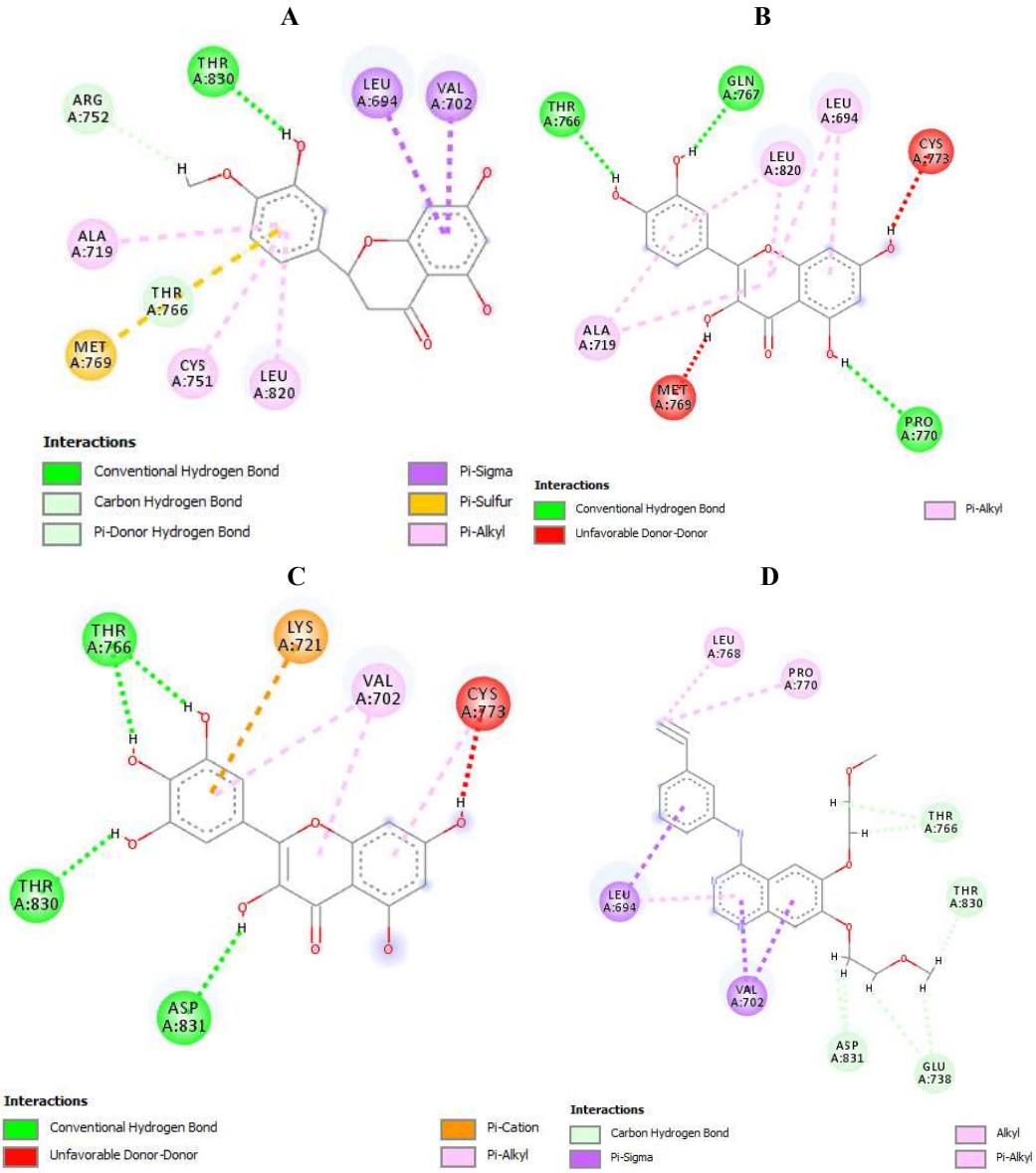

Fig. 2. Interactions between EGFR and (A). Hesperetin. (B). Quercetin. (C). Myricetin. (D). Erlotinib.

Molecular Dynamics Simulation

On the top hits with high binding energies, molecular dynamics simulations were run. RMSD was used to represent the anticipated conformational changes from the original structure across the simulation period. The RMSD is for measuring the degree of fluctuation of the protein when different putative drugs are docked to it. All docked protein structures equilibrated after 80 ns in terms of RMSD as shown in (Fig. 3). It is noteworthy that the EGFR-quercetin complex has RMSD much higher than other complexes of other drugs (After 80 ns, hesperetin: mean: 2.49 Å, SD: 0.12 Å; quercetin: mean: 11.2 Å, SD: 0.19 Å; myricetin: mean: 2.50 Å, SD: 0.11 Å; erlotinib: mean: 2.16 Å, SD: 0.20 Å), which possibly indicates that binding of quercetin destabilizes EGFR to a greater extent. Also, we noticed that the RMSD of the myricetin system is relatively higher than those of hesperetin and erlotinib in some periods during the simulation.

Furthermore, the RMSF is the measure of fluctuation in residue level (Fig. 4). The RMSF is relatively higher at the C- and N-terminals, which is an indication that they have more freedom to move at the end of the polypeptide chain. It is noticed that the quercetin-EGFR complex has an overall higher RMSF in almost every domain, agreeing with the RMSD result. The myricetin system exhibits slightly higher RMSF in residues 150-200, indicating that the increased RMSD of the EGFR-myricetin complex is influenced by this domain.

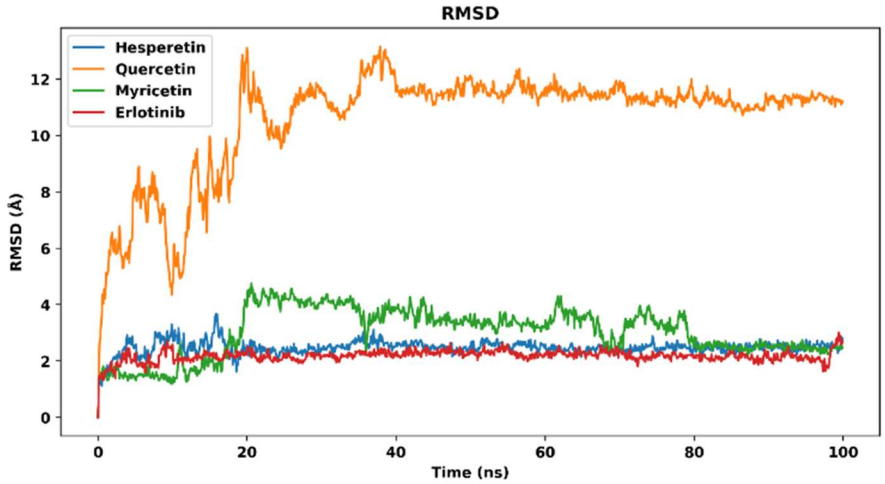

Fig. 3. RMSD plot of a) Erlotinib-EGFR, b) Quercetin-EGFR, c) Myricetin-EGFR, and d) Hesperetin-EGFR.

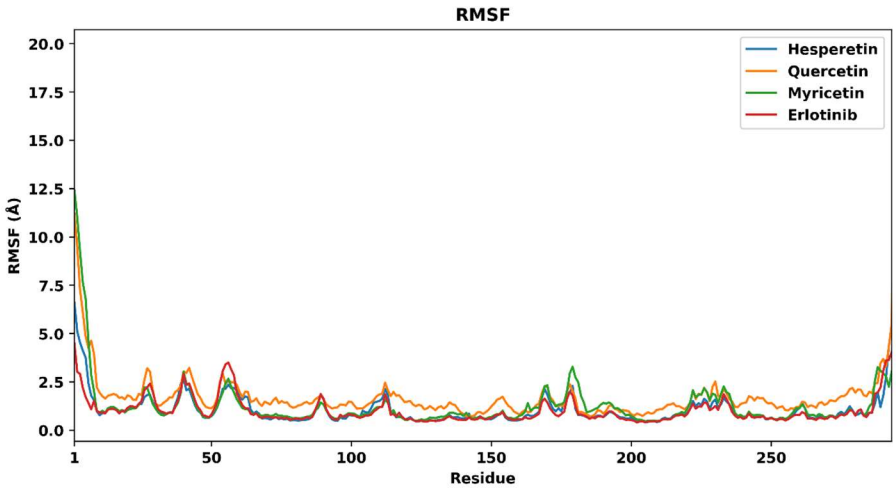

Fig. 4. RMSF plot of a) Erlotinib-EGFR, b) Quercetin-EGFR, c) Myricetin-EGFR, and d) Hesperetin-EGFR.

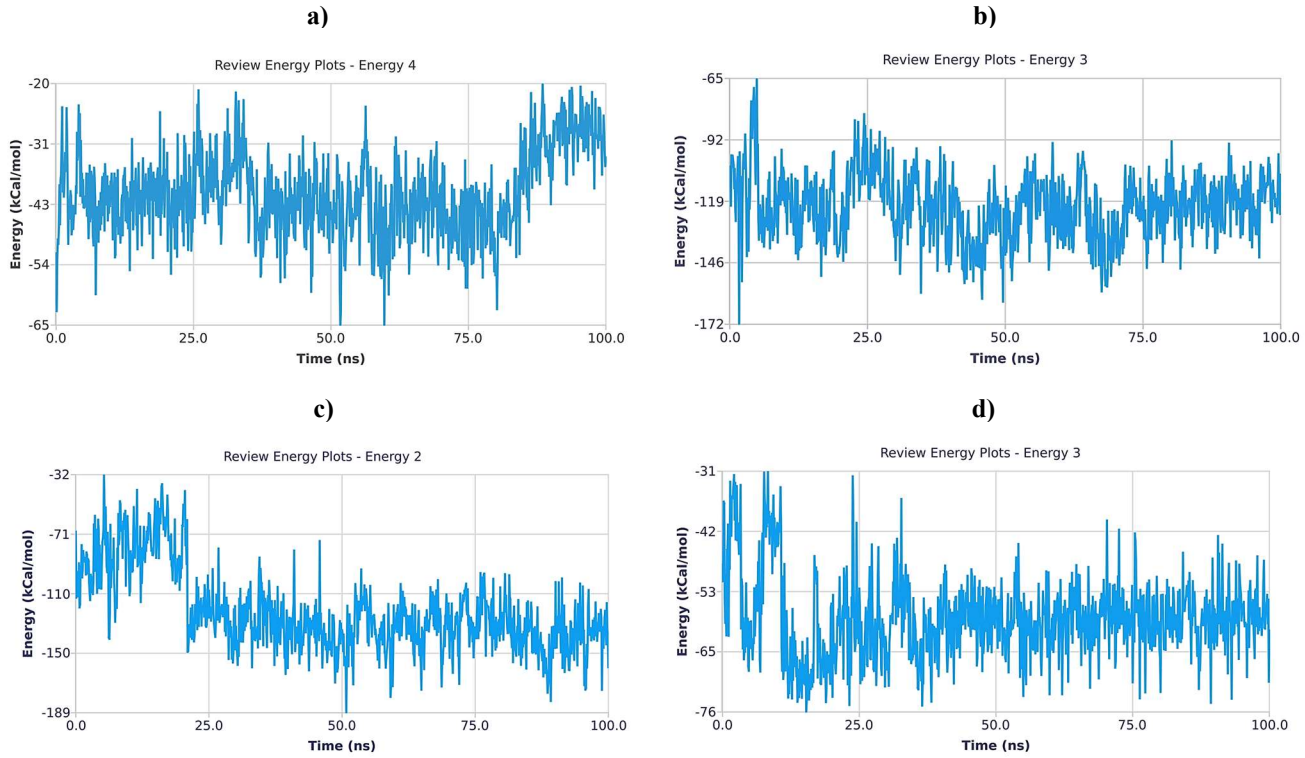

Fig. 5. Energy fluctuation plot of a) Erlotinib-EGFR, b) Quercetin-EGFR, c) Myricetin-EGFR, and d) Hesperetin-EGFR.

various drugs. The Rg values are similar for hesperetin, myricetin and erlotinib systems, but it is higher for the quercetin system, especially the time just after the beginning of the simulation, which indicates its lower degree of compactness (After 80 ns, hesperetin: mean: 19.71 Å, SD: 0.09 Å; quercetin: mean: 20.21 Å, SD: 0.16 Å; myricetin: mean: 19.72 Å, SD: 0.16 Å; erlotinib: mean: 19.56 Å, SD: 0.13 Å). In the RMSD analysis, we showed that the quercetin system fluctuated more, which agrees with the result of Rg that it is less compact, as shown in (Fig. 6).

The secondary structure shows that the 4 systems exhibit similar patterns. In residues 60-70, 100-130, and 200-290, there are mainly α-helices, while in residues 1-50, 75-100, and 125-175, there are mainly β-strands (Fig. 7). The percentages of α-helices are 29.79%, 30.09%, 30.82%, and 30.67% while those of β-strands are 17.01%, 14.69%, 16.67%, and 16.45% for hesperetin, quercetin, myricetin, and erlotinib systems, respectively. Overall, there are totals of 46.80%, 44.79%, 47.49%, and 47.11% of secondary structures in these systems respectively. It should be noted that the quercetin system has the lowest percentage of secondary structures, which could be the cause of its higher

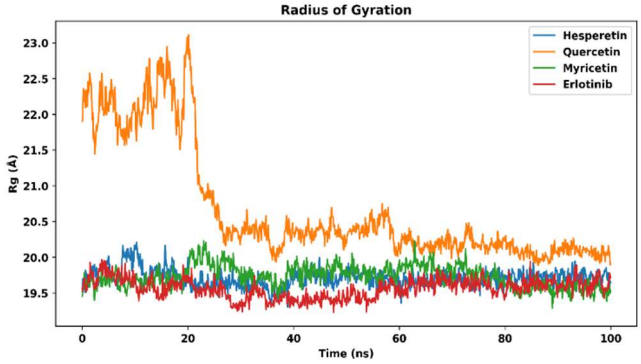

Fig. 6. Radius of Gyration plot of a) Erlotinib-EGFR, b) Quercetin-EGFR, c) Myricetin-EGFR, and d) Hesperetin-EGFR.

RMSD and Rg, the indications of higher fluctuations and lower compactness. Decomposing the percentages of secondary structures concerning time, we see that the ligands cause disruptions in the α-helices to the C-terminal in different degrees. Quercetin caused the most disruptions in that region among all systems.

Hesperetin

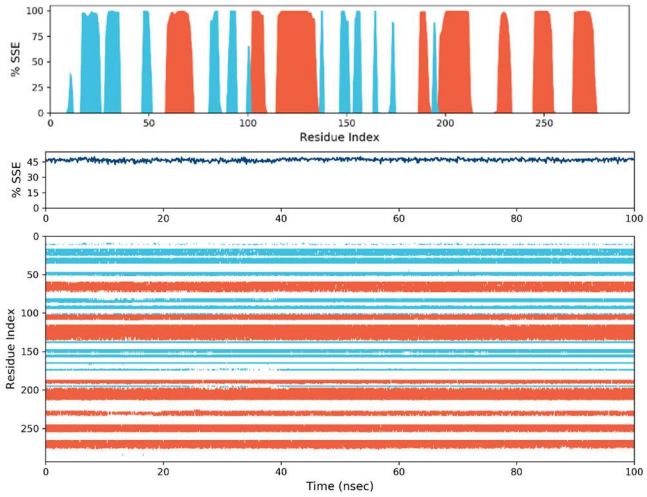

Quercetin

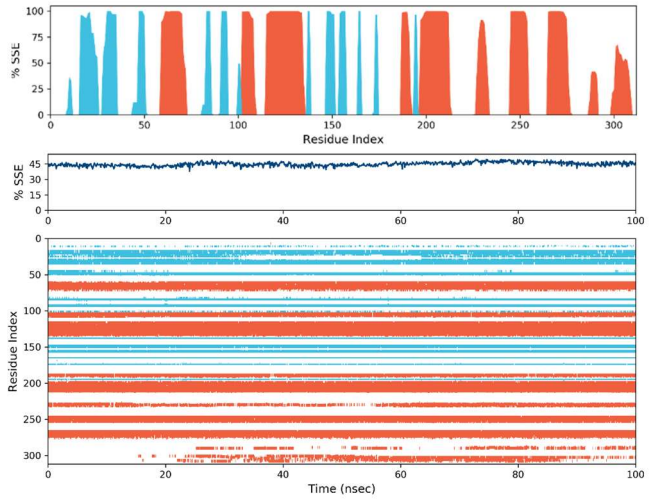

Myricetin

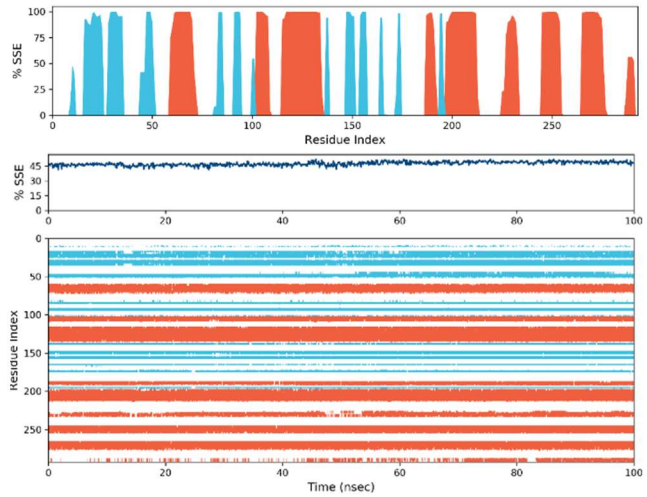

Erlotinib

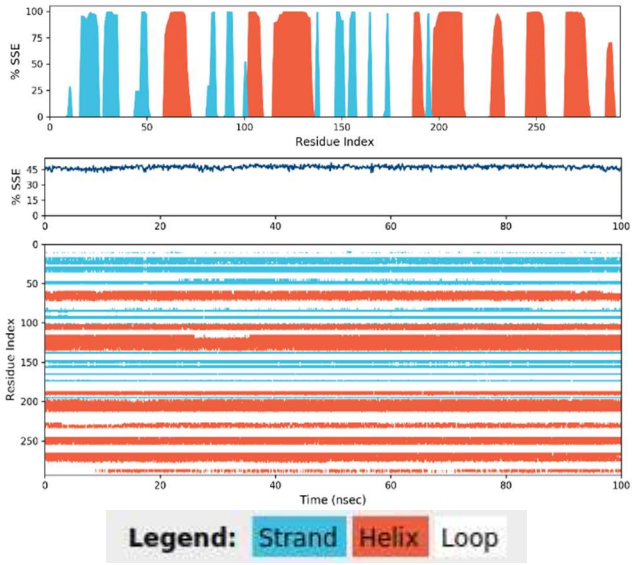

Fig. 7. The secondary structure plot of a) Hesperetin, b) Quercetin, c) Myricetin, and d) Erlotinib.

ADMET Properties

Pharmacokinetic ADMET properties were predicted using pkCSM to ensure the viability of the selected phytocompounds and Erlotinib. Table 2 shows the findings of the ADMET properties.

Absorption and distribution. A molecule that is absorbed by the human gastrointestinal system to less than 30% is termed poorly absorbed. Human oral absorption of the six chosen compounds was greater than 30%, implying that each substance was thoroughly absorbed. A volume of distribution (VDss) value logVDss of less than -0.15 indicates poor dispersion. All chemicals showed a VDss value greater than -0.15, indicating that rather than plasma, tissues can be where they are distributed.

Metabolism. Enzymatic metabolism is vital in the conversion of a substance, like a drug, as well as its biotransformation within the human body. All the substances tested were shown to be CYP2D6 substrates, as indicated in Table 2. Only Hesperetin, on the other hand, has been demonstrated to inhibit the cytochrome P450 subtypes CYP1A2, CYP2C19, CYP2C9, CYP2D6, and CYP3A4, suggesting potential metabolism in the liver.

Table 2. ADMET Properties of the 3 Selected Phytocompounds and Erlotinib

	Absorption	Distribution	Metabolism CYP							Excretion	Toxicity
	Intestinal Absorption (Human) (%absorbed)	VDss (human) (logl/Kg)	2D6	3A4	1A2	2C19	2C9	2D6	3A4	Total Clearance ((logml/min/kg)	Carcinogens
			Substrate		Inhibitor						
Hesperetin	77.875	-0.023	No	No	Yes	Yes	Yes	Yes	Yes	0.128	No
Quercetin	75.093	0.272	No	No	Yes	No	No	No	No	0.603	No
Myricetin	66.197	0.332	No	Yes	Yes	No	No	No	No	0.574	No
Erlotinib	96.052	0.09	No	Yes	No	Yes	Yes	No	Yes	0.578	No

VDss: volume of distribution at steady state. CYP: cytochrome P450.

Excretion and toxicity. The total clearance of the selected compounds is high, while that of Hesperetin is low but acceptable, indicating that it could be filtered in a combinational manner by hepatic and renal tissues. These compounds were also put through the Carcinogens test. The findings of the analysis were negative, showing that none of these compounds were mutagenic or carcinogenic. The toxicity test outcome reveals the safety of the examined compounds, which is highly advantageous in developing an effective drug.

According to the ADMET analysis, the chosen compounds, particularly Hesperetin, were in silico confirmed and might be employed as safer lead compounds in future studies.

Hesperetin, Quercetin, and Myricetin emerged as the top EGFR inhibitors among the five phytochemicals based on molecular docking studies. Hesperetin exhibited deep docking into the EGFR binding region, leading to favorable binding interactions and improved total scores and docking energies. Similar to Erlotinib, these three compounds penetrated the EGFR cavity, resulting in enhanced total scores, docking energies, and favorable binding interactions critical for stabilizing the docking complex. The present results suggest that these compounds, especially Hesperetin, have the potential to act as novel EGFR inhibitors. Furthermore, Hesperetin demonstrated greater stability and stronger inhibitory effects on the receptor protein compared to the others. ADMET analysis supported the safety of these compounds, particularly Hesperetin, making them promising lead compounds for future studies. This favorable toxicity profile is advantageous for developing effective drugs.

CONCLUSION

In the current study, several computational methodologies were used to investigate the anti-proliferative properties of five Caralluma europaea chemical compounds against the EGFR, which is a major protein in charge of the growth of pancreatic cancer and non-small cell lung cancer. Molecular docking and molecular dynamic simulation analysis suggest Hesperetin, Quercetin, and Myricetin as the most potent EGFR inhibitors among the five selected phytochemicals. The Hesperetin-EGFR combination was shown to be more stable. Subsequently, the stability of the three chosen phytochemical compounds along with the reference molecule was investigated using MD simulation at 100 ns. The results reveal that Hesperetin has high stability. The ADMET profiles of the selected phytocompounds were predicted in silico, and Hesperetin exhibited a favorable ADMET profile. Finally, the current findings suggest that Hesperetin has the potential to be a promising EGFR inhibitor for the prevention of pancreatic cancer and non-small cell lung cancer, and further in vitro and clinical studies may confirm its therapeutic potential.

ACKNOWLEDGEMENTS

We are thankful to the "Association Marocaine des Chimistes Théoriciens" (AMCT) for their valuable assistance regarding the programs.

REFERENCES

[1] Spinello, Z.; Fregnani, A.; Quotti Tubi, L.; Trentin, L.; Piazza, F.; Manni, S., Targeting Protein Kinases in Blood Cancer: Focusing on CK1α and CK2. *Int. J. Mol. Sci.*, **2021**, *22* (7), 3716. https://doi.org/10.3390/ijms22073716.

[2] Pfeifer, E.; Burchell, J. M.; Dazzi, F.; Sarker, D.; Beatson, R., Apoptosis in the Pancreatic Cancer Tumor Microenvironment-The Double-Edged Sword of Cancer-Associated Fibroblasts. *Cells*, **2021**, *10* (7), 1653. https://doi.org/10.3390/cells10071653.

[3] Carneiro, B. A.; El-Deiry, W. S., Targeting Apoptosis in Cancer Therapy. *Nat. Rev. Clin. Oncol.*, **2020**, *17* (7), 395-417. https://doi.org/10.1038/s41571-020-0341-y.

[4] Hassanein, S. S.; Ibrahim, S. A.; Abdel-Mawgood, A. L., Cell Behavior of Non-Small Cell Lung Cancer Is at EGFR and MicroRNAs Hands. *Int. J. Mol. Sci.*, **2021**, *22* (22), 12496. https://doi.org/10.3390/ijms222212496.

[5] Uribe, M. L.; Marrocco, I.; Yarden, Y., EGFR in Cancer: Signaling Mechanisms, Drugs, and Acquired Resistance. *Cancers*, **2021**, *13* (11), 2748. https://doi.org/10.3390/cancers13112748.

[6] Lin, S. -R.; Yeh, H. -L.; Liu, Y. -N., Interplay of Epidermal Growth Factor Receptor and Signal Transducer and Activator of Transcription 3 in Prostate Cancer: Beyond Androgen Receptor Transactivation. *Cancers*, **2021**, *13* (14), 3452. https://doi.org/10.3390/cancers13143452.

[7] Cox, G.; Vyberg, M.; Melgaard, B.; Askaa, J.; Oster, A.; O'Byrne, K. J., Herceptest: HER2 Expression and Gene Amplification in Non-Small Cell Lung Cancer. *Int. J. Cancer*, **2001**, *92* (4), 480-483. https://doi.org/10.1002/ijc.1214.

[8] Lefebvre, C.; Allan, A. L., Anti-Proliferative and Anti-Migratory Effects of EGFR and c-Met Tyrosine Kinase Inhibitors in Triple Negative Breast Cancer Cells. *Precis. Cancer Med.*, **2021**, *4* (0). https://doi.org/10.21037/pcm-20-62.

[9] Seshacharyulu, P.; Ponnusamy, M. P.; Haridas, D.; Jain, M.; Ganti, AparK.; Batra, S. K., Targeting the EGFR Signaling Pathway in Cancer Therapy. *Expert. Opin. Ther. Targets*, **2012**, *16* (1), 15-31. https://doi.org/10.1517/14728222.2011.648617.

[10] Wang, Z.; Kim, J.; Zhang, P.; Galvan Achi, J. M.; Jiang, Y.; Rong, L., Current Therapy and Development of Therapeutic Agents for Lung Cancer. *Cell Insight*, **2022**, 100015. https://doi.org/10.1016/j.cellin.2022.100015.

[11] Shrihastini, V.; Muthuramalingam, P.; Adarshan, S.; Sujitha, M.; Chen, J. -T.; Shin, H.; Ramesh, M., Plant Derived Bioactive Compounds, Their Anti-Cancer Effects and *In Silico* Approaches as an Alternative Target Treatment Strategy for Breast Cancer: An Updated Overview. *Cancers*, **2021**, *13* (24), 6222. https://doi.org/10.3390/cancers13246222.

[12] Newman, D. J.; Cragg, G. M., Natural Products as Sources of New Drugs over the Last 25 Years. *J. Nat. Prod.*, **2007**, *70* (3), 461-477. https://doi.org/10.1021/np068054v.

[13] Ng, C. X.; Affendi, M. M.; Chong, P. P.; Lee, S. H., The Potential of Plant-Derived Extracts and Compounds to Augment Anticancer Effects of Chemotherapeutic Drugs. *Nutr. Cancer*, **2022**, *74* (9), 3058-3076. https://doi.org/10.1080/01635581.2022.2069274.

[14] Adnan, M.; Jan, S.; Mussarat, S.; Tariq, A.; Begum, S.; Afroz, A.; Shinwari, Z. K., A Review on Ethnobotany, Phytochemistry and Pharmacology of Plant Genus Caralluma R. Br. *J. Pharm. Pharmacol.*, **2014**, *66* (10), 1351-1368. https://doi.org/10.1111/jphp.12265.

[15] Amrati, F. ez-zahra; Bourhia, M.; Slighoua, M.; Ibnemoussa, S.; Bari, A.; Ullah, R.; Amaghnouje, A.; Di Cristo, F.; El Mzibri, M.; Calarco, A.; *et al*. Phytochemical Study on Antioxidant and Antiproliferative Activities of Moroccan Caralluma Europaea Extract and Its Bioactive Compound Classes. *Evid. Based Complement. Alternat. Med.*, **2020**, *2020*, e8409718. https://doi.org/10.1155/2020/8409718.

[16] Tirado-Rives, J.; Jorgensen, W. L., Performance of B3LYP Density Functional Methods for a Large Set of Organic Molecules. *J. Chem. Theory Comput.*, **2008**, *4* (2), 297-306. https://doi.org/10.1021/ct700248k.

[17] Stamos, J.; Sliwkowski, M. X.; Eigenbrot, C., Structure of the Epidermal Growth Factor Receptor

Kinase Domain Alone and in Complex with a 4-Anilinoquinazoline Inhibitor*. *J. Biol. Chem.*, **2002**, *277* (48), 46265-46272. https://doi.org/10.1074/jbc.M207135200.

[18] El Khatabi, K.; El-mernissi, R.; Aanouz, I.; Ajana, M. A.; Lakhlifi, T.; Shahinozzaman, M.; Bouachrine, M., Benzimidazole Derivatives in Identifying Novel Acetylcholinesterase Inhibitors: A Combination of 3D-QSAR, Docking and Molecular Dynamics Simulation. *Phys. Chem. Res.*, **2022**, *10* (2), 237-249. https://doi.org/10.22036/pcr.2021.277306.1895.

[19] Trott, O.; Olson, A. J., AutoDock Vina: Improving the Speed and Accuracy of Docking with a New Scoring Function, Efficient Optimization and Multithreading. *J. Comput. Chem.*, **2010**, *31* (2), 455-461. https://doi.org/10.1002/jcc.21334.

[20] El Khatabi, K.; Aanouz, I.; El-mernissi, R.; Khaldan, A.; Ajana, M. A.; Bouachrine, M.; Lakhlifi, T., 3D-QSAR and Molecular Docking Studies of p-Aminobenzoic Acid Derivatives to Explore the Features Requirements of Alzheimer Inhibitors. *Orbital Electron. J. Chem.*, **2020**, *12* (4), 172-181. https://doi.org/10.17807/orbital.v12i4.1467.

[21] EL-Mernissi, R.; EL Khatabi, K.; Khaldan, A.; El Mchichi, L.; Ajana, M. A.; Lakhlifi, T.; Bouachrine, M., Design of New 3, 5-Disubstituted Indole as Hematological Anticancer Agents Using 3D-QSAR, Molecular Docking and Drug-Likeness Studies. *Mater. Today Proc.*, **2021**, *45*, 7608-7614. https://doi.org/10.1016/j.matpr.2021.03.080.

[22] Li, X.; Chu, Z.; Du, X.; Qiu, Y.; Li, Y., Combined Molecular Docking, Homology Modelling and Density Functional Theory Studies to Modify Dioxygenase to Efficiently Degrade Aromatic Hydrocarbons. *RSC Adv.*, *9* (20), 11465-11475. https://doi.org/10.1039/c8ra10663k.

[23] Alesawy, M. S.; Elkaeed, E. B.; Alsfouk, A. A.; Metwaly, A. M.; Eissa, I. H., *In Silico* Screening of Semi-Synthesized Compounds as Potential Inhibitors for SARS-CoV-2 Papain-like Protease: Pharmacophoric Features, Molecular Docking, ADMET, Toxicity and DFT Studies. *Molecules*, **2021**, *26* (21), 6593. https://doi.org/10.3390/molecules26216593.

[24] Discovery Studio Predictive Science Application| Dassault Systèmes BIOVIA https://www.3dsbiovia.com/products/collaborative-science/biovia-discovery-studio/ (accessed Feb 6, 2020).

[25] DeLano, W. L., Pymol: An Open-Source Molecular Graphics Tool. *CCP4 Newsl. Protein Crystallogr.*, **2002**, *40* (1), 82-92.

[26] Ononamadu, C. J.; Ibrahim, A., Molecular Docking and Prediction of ADME/Drug-Likeness Properties of Potentially Active Antidiabetic Compounds Isolated from Aqueous-Methanol Extracts of Gymnema Sylvestre and Combretum Micranthum. *BioTechnologia*, **2021**, *102* (1), 85-99. https://doi.org/10.5114/bta.2021.103765.

[27] Pires, D. E. V.; Blundell, T. L.; Ascher, D. B., pkCSM: Predicting Small-Molecule Pharmacokinetic and Toxicity Properties Using Graph-Based Signatures. *J. Med. Chem.*, **2015**, *58* (9), 4066-4072. https://doi.org/10.1021/acs.jmedchem.5b00104.

[28] El Khatabi, K.; Kumar, S.; El-Mernissi, R.; Singh, A. K.; Ajana, M. A.; Lakhlifi, T.; Bouachrine, M., Novel Eubacterium Rectale Inhibitor from Coriandrum Sativum L. for Possible Prevention of Colorectal Cancer: A Computational Approach. *J. Biomol. Struct. Dyn.*, **2022**, 1-15. https://doi.org/10.1080/07391102.2022.2134210.

[29] Rehman, H. M.; Sajjad, M.; Ali, M. A.; Gul, R.; Irfan, M.; Naveed, M.; Bhinder, M. A.; Ghani, M. U.; Hussain, N.; Said, A. S. A.; *et al.* Identification of NS2B-NS3 Protease Inhibitors for Therapeutic Application in ZIKV Infection: A Pharmacophore-Based High-Throughput Virtual Screening and MD Simulations Approaches. *Vaccines*, **2023**, *11* (1), 131. https://doi.org/10.3390/vaccines11010131.

[30] Gul, R.; Hanif, M. U.; Gul, F.; Rehman, H. M.; Saleem, M.; Ahmad, M. S.; Mirza, M. U., Molecular Cloning, Expression, Sequence Characterization and Structural Insight of Bubalus Bubalis Growth Hormone-Receptor. *Mol. Biotechnol.*, **2023**, *65* (7), 1062-1075. https://doi.org/10.1007/s12033-022-00612-y.

[31] Shinwari, K.; Rehman, H. M.; Liu, G.; Bolkov, M. A.; Tuzankina, I. A.; Chereshnev, V. A., Novel Disease-Associated Missense Single-Nucleotide

Polymorphisms Variants Predication by Algorithms Tools and Molecular Dynamics Simulation of Human TCIRG1 Gene Causing Congenital Neutropenia and Osteopetrosis. *Front. Mol. Biosci.*, **2022**, *9*, 879875. https://doi.org/10.3389/fmolb.2022.879875.